Available online at www.sciencedirect.com
SCIENCE DIRECT
Journal of Photochemistry and Photobiology A: Chemistry 181 (2006) 158–165
Journal of Photochemistry and Photobiology A:Chemistry
www.elsevier.com/locate/jphotochem

Improving ultraviolet light transmission in a packed-bed photoelectrocatalytic reactor for removal of oxalic acid from wastewater

Taicheng An [a,*], Ya Xiong [b], Guiying Li [a], Xihai Zhu [b], Guoying Sheng [a], Jiamo Fu [a,*]

[a] *State Key Laboratory of Organic Geochemistry, Guangdong Key Laboratory of Environmental Protection and Resources Utilization, Guangzhou Institute of Geochemistry, Chinese Academy of Sciences, Guangzhou 510640, China*
[b] *School of Chemistry and Chemical Engineering, Zhongshan University, Guangzhou 510275, China*

Received 31 October 2004; received in revised form 7 April 2005; accepted 19 November 2005
Available online 27 December 2005

Abstract

A novel three-dimensional electrode–hollow quartz tube photoelectrocatalytic reactor was designed and characterized by the photocurrent enhancement and COD removal efficiency, and the packed-bed photoelectrocatalytic reactor was used to investigate the feasibility of synergetic photoelectrocatalytic degradation of oxalic acid. By comparison of the COD removal efficiencies of three processes, direct electrooxidation, photocatalysis, and photoelectrocatalysis, the results showed that not only a significant photoelectrochemical synergetic effect, but also good photocatalytic efficiency, were observed in the photoelectrocatalytic reactor. It was found that successful design of the photoelectrocatalytic reactor by introducing the hollow quartz tubes into the three-dimensional electrode-packed-bed photoelectrocatalytic reactor presented a good solution to the drawbacks for poorly treating the high concentration and low-transmittance wastewater by photocatalytic technology.

Keywords: Photoelectrocatalytic reactor; Photocatalytic enhancement; Three-dimensional electrode; Synergetic effect; Oxalic acid

1. Introduction

The widespread pollution of drinking water or effluents with hazardous and biostable organic compounds demands an increasing effort towards the development of technologies for the cleanup of such wastewater. Alternative processes for the treatment of wastewater and drinking water are the so-called advanced oxidation processes (AOPs). Heterogeneous photocatalytic oxidation of organic pollutants is one of potential AOPs. The appeal of this technology is the prospect of complete mineralization of the pollutants into harmless compounds [1,2]. However, conventional powder catalysts in a slurry photocatalytic reactor suffered from disadvantages in stirring during the reaction and in separation after the reaction in scale-up system [3]. This made the process very complicated, meanwhile the post-treatment cost also increased significantly. This problem presents a major drawback for the commercial application of slurry photocatalytic reactor to treating wastewater. Alternatively, the catalyst may be immobilized onto a suitable solid inert support and used as immobilized film form, which eliminated the need of removing the catalyst from water. Unfortunately, when the catalyst was immobilized there was a decrease in the available surface area for the reaction since the catalyst must adhere to the solid support unless the substrate was UV transparent, thus the reactor design was limited by the optical absorption constraints. Moreover, the catalytic efficiency in the immobilizing film reactor was very small, just a fraction of 10 compared with the slurry reactor [4]. In order to present a good solution to these problems, Peill and Hoffmann [5,6] had constructed a fixed-bed photocatalytic reactor system employing a fiber-optic cable. This successful design of the reactor not only greatly minimize heat buildup problem, but also give a higher quantum yield of two folds to Hofstadler's reactor [7]. However, Ray pointed out that the manufacture of optical fiber and auxiliary facilities

* Corresponding authors. Tel.: +86 20 85291501; fax: +86 20 85290706.
E-mail address: antc99@gig.ac.cn (T. An).

1010-6030/$ – see front matter © 2005 Elsevier B.V. All rights reserved.
doi:10.1016/j.jphotochem.2005.11.019

cost too much to apply it to wastewater treatment in practical [8].

Recently, the photoelectrochemical technology with external electric field appears to be an efficient approach to improve the photocatalytic efficiencies and becomes a research front of photocatalytic degradation of organic pollutants. But, in most of the photoelectrocatalytic systems, the applied anodic bias potential is always lower than that of object organic pollutant so that no direct electrochemical oxidations interfere with the photocatalytic mechanism [9–11]. But there are a few researches to discuss the hybrid photoelectrocatalytic technology under high electric field [12–14], and two novel hybrid photoelectrocatalytic reactors, a three-dimensional electrode–slurry photocatalytic reactor [12,14] and a three-dimensional electrode–packed-bed photocatalytic reactor [13,15], were developed for the degradation of organic pollutants in our group. Unfortunately, no matter what kind of reactors, both the designed reactors had their inherent drawbacks in the three-dimensional electrode reactors. That is, three-dimensional electrode reactor must be the packed-bed reactor which has a unique problem that the UV light distribution is not considerable uniform [12,16]. In order to overcome this problem, we introduced the hollow quartz tubes as a means of light transmitter and distributor into the packed-bed photocatalysts, and developed a novel three-dimensional electrode–hollow quartz tube photoelectrocatalytic reactor for degrading organic pollutants. This distributive mode of UV light in photocatalytic reactor will allow UV light to pass better through the packed-bed photocatalyst and has a larger illuminated area than packed-bed photocatalytic reactor. As a result, the design of the novel photoelectrocatalytic reactor can not only greatly decrease the manufacturing cost, but also successfully solve the drawback of light distribution which existed in packed-bed photocatalytic and photoelectrocatalytic reactor.

2. Experimental

2.1. Materials

Sixty quartz tubes with outside diameter of 4 mm and inside diameter of 2.8 mm were arrayed as four lines and used as a transmission facility of UV light. The micropore titanium plate was used as both cathode and anode after disposed with diluted sulfuric acid and then washed with deionized water twice, respectively. The available surface area of both electrodes is 5 cm^{-2} (2.5 cm × 2 cm), respectively. Titanium dioxide Degussa P25 is composed mainly of anatase (ca. 70%). Oxalic acid was analytic grade reagent, and the solutions were prepared with deionized water to the concentration of 50 mmol L^{-1} (COD: ca. 816.6 ppm; pH value: 1.4). All other reagents were analytic grade.

2.2. Preparation of granular titanium-supported TiO_2

A 300-ml aqueous suspension containing 15 g of TiO_2 was agitated for 4 h and sonicated for 30 min, and then used for coating granular titanium. Upon cleanup by sonication in ethanol and deionzed water, 300 g of 100 mesh granular titanium were immerged in the suspension solution. The mixture was continuously mechanically agitated for 2 h. The resulting mixtures were separated by filtration, dried at 100 °C and then calcined for 4 h in an oven at 400 °C. Loading, drying, and calcining procedures were repeated twice. After being washed with deionzed water, the coating of granular titanium was dried at 120 °C and weighed. The scanning electron microscopy (SEM) showed that the coated material was covered well by a deep coat of TiO_2, and the quantity of TiO_2 coating on granular titanium was about 0.082 g g^{-1}. The granular titanium coated by TiO_2 was used as the filler both for the three-dimensional electrode and for the packed-bed photocatalyst in this photoelectrocatalytic reactor.

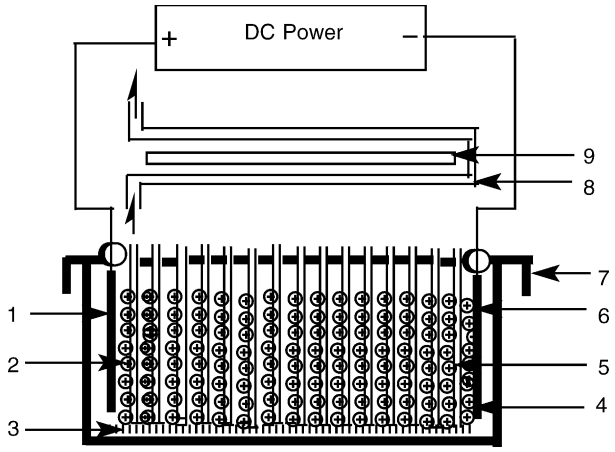

Fig. 1. Schematic of photoelectrocatalytic reactor set-up: (1) anode; (2) TiO_2-coated Ti particles; (3) micropore plate; (4) cathode; (5) hollow quartz tubes; (6) glass cell; (7) aluminum foil cover; (8) double-walled quartz tube; (9) high pressure mercury lamp.

2.3. Photoelectrocatalytic reactor

The set-up is a couple of three-dimensional electrode electrochemical reactor with a packed-bed photocatalytic reactor employed the hollow quartz tube as a transmission facility of UV light; the schematic diagram of photoelectrocatalytic reactor is shown in Fig. 1. The reaction set-up consisted of four parts: a 500-W high-pressure mercury lamp with a reflector; a double-walled cooling quartz tube with a 5.0-mm-thick cooling water; a batch glass reactor (7 cm × 3 cm × 3 cm) with 60 hollow tubes and 50 g packed material of TiO_2-coated granular titanium. In this experiment, the packed material was used both for the photocatalyst of packed-bed photocatalytic reactor and for the particle electrode of the three-dimensional electrode electrochemical reactor. The high-pressure mercury lamp was located 8 cm above the reactor and placed in the cooling quartz tube with a cooling water flow (650 mL min^{-1}) to maintain reaction isothermality. Compressed air was bubbled upward through the gas distributor equipped at the bottom of the reactor in all experiments.

2.4. Apparatus and analysis

Absorption spectra of oxalic acid were recorded with a mode UV-PC2501 spectrophotometer (SHIMASZU, Japan). Current

was measured with a computerized CHI650A electrochemical system (Shanghai, China), which was also used as a potentiostat in the electrochemical experiments. Scanning electron discographies were obtained on a HITACHI S520 mode reflection electronic microscope. X-ray diffraction (XRD) was performed using D/Max-IIIA Diffratometer (Rigaku Corporation, Japan) with radiation of Cu target (Kα 1, $\lambda = 1.54056$ nm) to determine the crystal phase composition of the coated material at room temperature. And Millipore Disks (0.45 μm) were used to remove particulate mass of the colloid solution before analysis, and chemical oxygen demand (COD) was employed to reflect the amount of oxalic acid in the sample and measured with potassium dichromate.

2.5. Recommended procedure

Thirty millilitres of deionized water was added into the reactor and conducted 10 min for immersion of coated material before photoelectrochemical degradation. And then, 20 mL of synthetic wastewater containing oxalic acid was fed into the reactor after the residual immersion water was removed completely. The reactor was timed starting when the dc power, illumination and compressed air supply were switched on. With a 0.06 $m^3\ h^{-1}$ sparged air, 30.0 V direct current and illumination, the photoelectrochemical procedure was carried out for 60 min in the reactor for each batch run, then the sample solutions were collected, separated with centrifuge and filtered through a Millipore (0.45 μm) membrane for optical absorption and COD analyses.

3. Results and discussion

3.1. Characterization of immobilized photoelectroatalyst

The XRD figure presented in Fig. 2 showed that the crystal phase did not change after the P25 TiO_2 was immobilized onto the granular titanium because the heat treatment temperature was only 400 °C and lower than the change temperature of crystal phase of TiO_2. Thus, there are also anatases and rutile phases in coated photocatalyst, and has the same ratio as

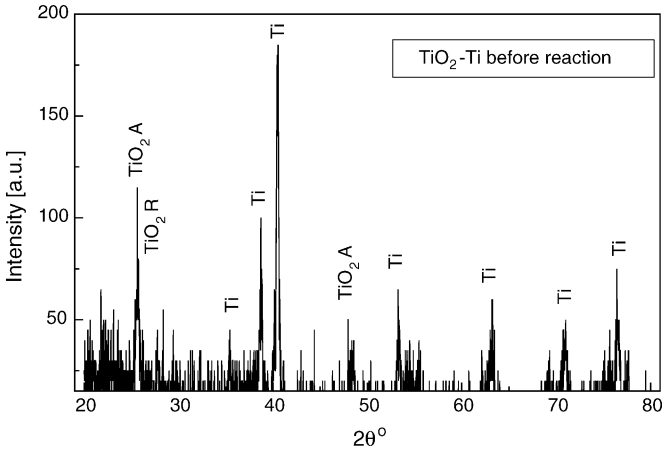

Fig. 2. XRD spectrum of immobilized photoelectrocatalyst.

P25 TiO_2. The SEM technology was also employed to observe the surface morphologies of coated photocatalyst. The granular titanium coated without or with Degussa P25 TiO_2 was shown in Fig. 3. It was found that the Degussa P25 TiO_2 was distributed uniformly on the supported granular titanium, and the substrate was completely covered by a coat of TiO_2. SEM images showed that the TiO_2 particle had an aggregation effect in the process of immobilization, and had a diameter range of about 50–100 nm, greater than that of 30 nm of original P25 TiO_2.

3.2. Current–voltage characteristics

The photocurrent–voltage behavior can directly reflect the competition reactions between the hole mediated and electron consuming [9–11]. Thus, one can minimize charge recombination with the application of external electric field to the TiO_2 electrode because the application of external electric field to the photocatalytic systems can efficiently provide a potential gradient to drive away the photogenerated holes and electrons in different directions. Also, the magnitude of the photocurrent is one of the major parameters characterizing photoelectrochemical reactor. Many research groups have extensively investigated

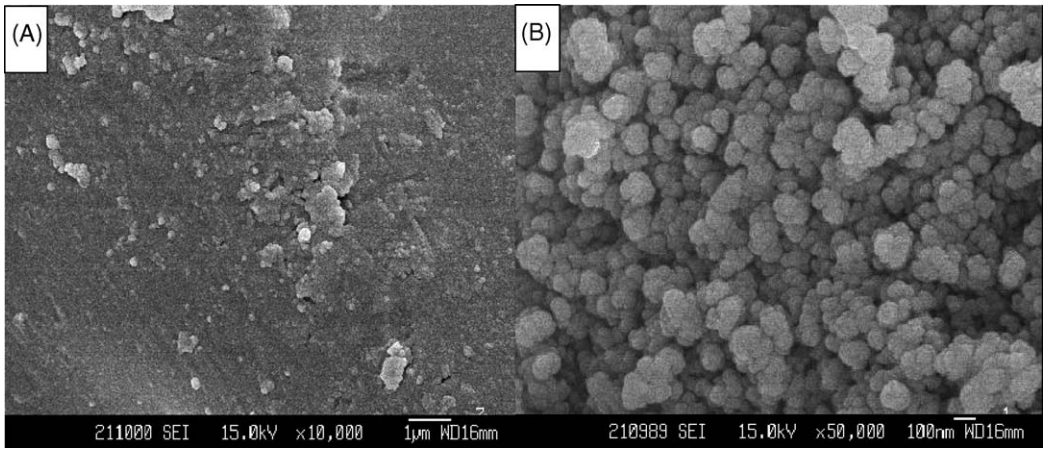

Fig. 3. SEM figure of substrate and immobilized photoelectrocatalyst granular titanium: (A) without coating P25 and (B) with coating P25.

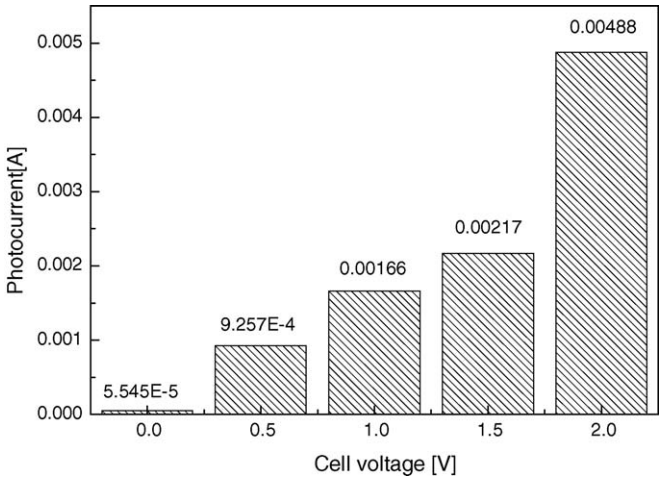

Fig. 4. Dependence of the cell voltages on photocurrent.

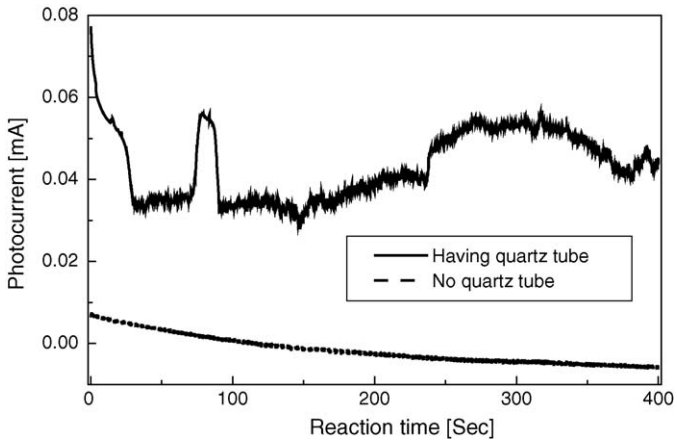

Fig. 5. Photocurrent curves for two reactors with or without hollow quartz tubes.

the photocurrent in the slurry and thin film photoelectrochemical reactors [17–22]. Kraeutler and Bard [23] and other researchers [19,24] have found that the photocurrent is very small and lower than 0.2 μA, although the slurry electrode has the great advantage of good mass-transfer. However, for the immobilized thin film reactor, the photocurrent is much higher than that of the slurry reactors [18,21,22,25]. In the present experiment, a high photocurrent, about 55.5 μA, was also observed in the three-dimensional electrode–parked-bed photoelectrocatalytic reactor, which is about 4.4 folds more than that of the reported three-dimensional electrode–slurry photoelectrocatalytic reactor [14]. It is indicated that the recombination of photogenerated holes and electrons substantially decreased by application of external electric field to the photocatalytic system. And this also may be an evidence of a synergic effect between photochemical and electrochemical process in the photoelectrocatalytic reactor. Furthermore, it may be imply that this photoelectrocatalytic reactor has a high efficiency for degrading organic pollutants.

Byrne and Eggins [26] have also investigated the potential dependence of photocurrent in the presence of oxalate. It was found that the onset of anodic photocurrent was ca. −0.9 V, the photocurrent rose sharply up in the oxalate solution with increasing positive bias up to ca. −0.5 V. In the present reactor, the current–voltage characteristics at various cell voltages were also investigated, and the results were also shown in Fig. 4. Seen from the figure, the photocurrent increased significantly with increase in the applied voltage. For example, when the applied voltages were 0.5 and 2.0 V, respectively, the photocurrents were 0.92 and 4.88 mA, respectively. The results showed that the higher the applied voltage is, the stronger the capturing ability to photogenerated electrons by external electric field is. This phenomenon was also observed both in the slurry and packed-bed photoelectrocatalytic reactor previously reported by our group [3,14]. This may be interpreted that with the increase of the applied voltage the potential gradient between two electrodes became much larger resulting in the decrease of the recombination rate of photogenerated electrons and holes.

In order to completely understand the effect of hollow quartz tubes assembled in the photoelectrocatalytic reactor, the photocurrent changes in the photoelectrocatalytic process with or without hollow quartz tubes were also measured in the presence of 50 mmol L^{-1} oxalic acid, and the resulting current–voltage profiles were shown in Fig. 5. It is found that 55.5 and 7.2 μA photocurrent were obtained with or without hollow quartz tubes in the two photoelectrocatalytic reactors, respectively. Moreover, both photocurrents decreased gently with increase in the reaction time. But the former is always higher than the latter, which indicated that the hollow quartz tubes played an important role in the light transmission in the photoelectrochemical reactor. That is, hollow quartz tubes could commendably improve the distribution of UV light in the packed-bed photoelectrocatalytic reactor.

Oxalic acid is a strong reductive electron donor having a redox couple $H_2C_2O_4$ (aq)/CO_2 (g) of −0.49 V referenced with normal hydrogen electrode, and can be irreversiblely combined with photogenerated holes or resulted hydroxyl radicals ($^{\bullet}$OH), inhibiting the recombination of photogenerated electrons and holes, thereby significantly enhancing the photocatalytic efficiencies of organic pollutants [27]. Thus, the current changes in the photoelectrocatalytic reactor were also measured in the presence or absence of 50 mmol L^{-1} oxalic acid, and the results were shown in Fig. 6. It is noted that the photocurrent was very small and near 0 V in the absence of oxalic acid, while the photocurrent increased rapidly when the oxalic acid solution was added into the reactor. The increase in the photocurrent may be interpreted by the fact that oxalic acid had a stronger capturing effect for photogenerated holes, and remarkably inhibited the recombination of photogenerated electrons and holes, thus the photocurrent could be strongly increased. The photocurrent–time change characteristics between various cell voltages and reaction times in three-dimensional electrode–parked-bed photoelectrocatalytic reactor were also measured in the presence of 50 mmol L^{-1} oxalic acid; the profiles are shown in Fig. 7. It is noted from the figure that all photocurrent decrease continuously with the increase of time. This means that the photocurrent decreased as oxalic acid was degraded in the solution. The pho-

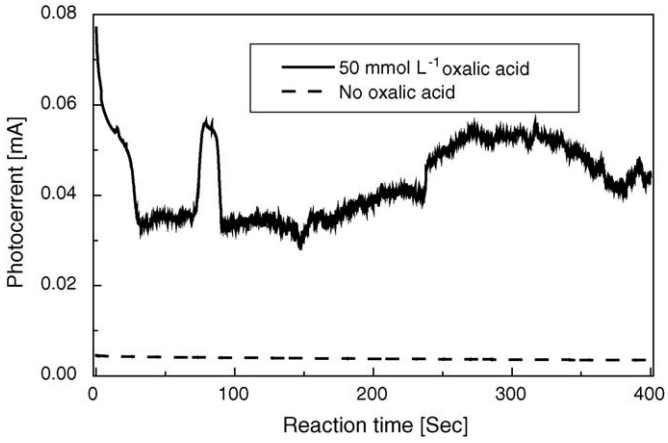

Fig. 6. Photocurrent change curves in the presence or absence of oxalic acid.

tocurrent decrease trend with the increase of reaction time was very similar to the results reported by Candal et al. [28] and our group [3]. Furthermore, the photocurrent decreases much faster at high cell voltage than that at low cell voltage. This also denoted that the higher the cell voltage was, the faster the degradation rate of oxalic acid was.

3.3. The effect of hollow quartz tubes in photoelectrocatalytic reactor

From above-mentioned, the packed-bed reactors were found to have a unique drawback, that the UV light distribution was not considerable uniform [12,16]. Thus, we employed the hollow quartz tube as a means of UV light transmitter and distribution throughout the photoelectrocatalytic reactor volume in this reactor. In order to completely understand the role of hollow quartz tubes in the photoelectrcatalytic reactor, the UV light intensity at desired interval depth of two photoelectrocatalytic reactors with or without hollow quartz tubes were investigated, respectively; the profiles are shown in Fig. 8. It is clear that the hollow quartz tubes have an apparent light transmission effect in the packed-bed photoelectrocatalytic reactor, and the UV light distribution in the photoelectrocatalytic reactor was substantially improved by using the hollow quartz tubes as a

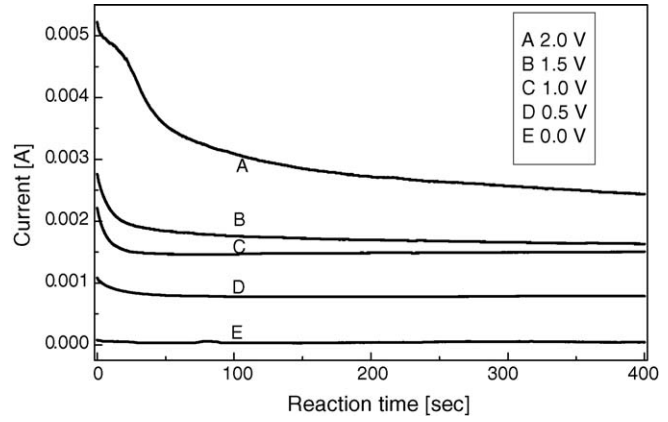

Fig. 7. Effect of reation time on photocurrents.

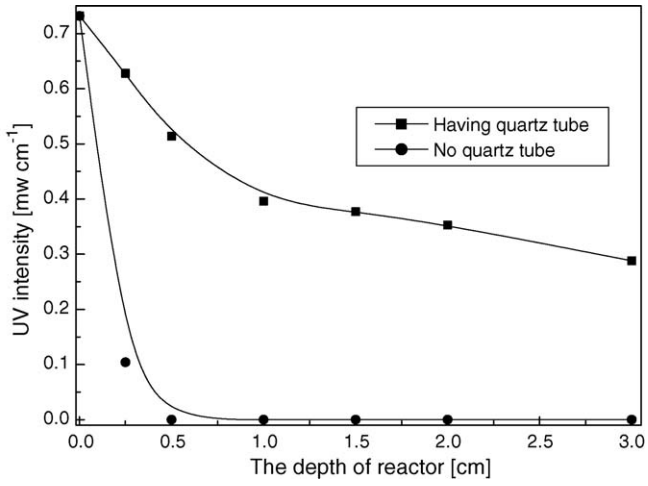

Fig. 8. UV light intensity for two reactors with and without quartz tubes.

UV light transmitter. Although the intensity of UV light on the surface of reaction solution was achieved at the average of 0.732 mW cm^{-2} with the highest peak at 365 nm in both reactors, the UV light intensity decreased dramatically in both reactors with the increase of the tube depth. Moreover, the UV light intensity in the photoelectrocatalytic reactor without the quartz tubes decreased more rapidly than that of the reactor with the quartz tubes. The UV light intensity reached only 0.104 and 0.000 mW cm^{-2} at the depth of 0.25 and 0.50 cm, respectively, in the reactor without the hollow quartz tubes, while the values were 0.628 and 0.514 mW cm^{-2} in the photoelectrocatalytic reactor in presence of the hollow quartz tubes. Moreover, there was also 0.288 mW cm^{-2} of UV light intensity at the bottom of the reactor with the hollow quartz tubes at the depth of 3.0 cm. So it can be concluded that the UV light transmission and distribution was substantially improved by introducing the hollow quartz tubes in the packed-bed photoelectrocatalytic reactor. Thus, it may be expected that the reactor with the hollow quartz tubes has higher COD removal efficiency for organic pollutants than the other reactor because of the good UV light distribution in the reactor.

So, in order to discuss the correlation between the distribution of UV light in the reactor and the reaction efficiencies of COD removal, the removal of oxalic acid from wastewater by photoelectrocatalytic process was carried out with or without hollow quartz tubes and the results are shown in Fig. 9. From the figure, we can see that the photoelectrocatalytic reactor in absence of hollow quartz tubes had a modest capacity for COD removal from the solutions. This may be due to the enhancement effect of three-dimensional electrodes on the photocatalytic system. When the photoelectrocatalytic degradation was consecutively conducted for five runs the COD removal values were 687.1, 617.0, 536.5, 484.0, and 421.0 mg L^{-1}, respectively. This indicated that though the distribution and transmission of UV light were very poor in the photoelectrocatalytic reactor, there is a satisfactory COD removal when no hollow quartz tubes were applied. However, in the presence of hollow quartz tubes, when the photoelectrocatalytic degradation was consecutively conducted for five runs the COD removal values were

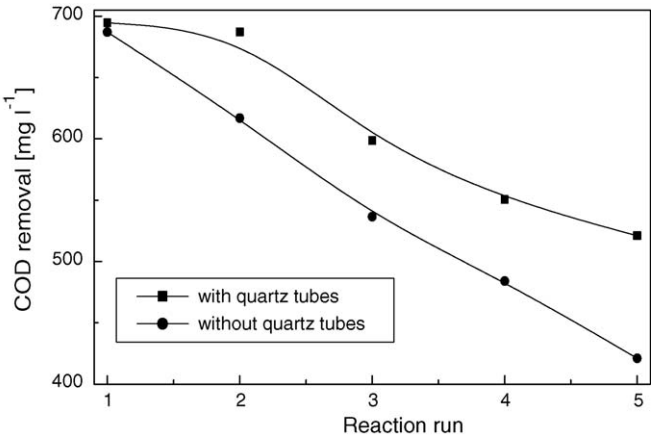

Fig. 9. COD removal for two reactors with and without quartz tubes.

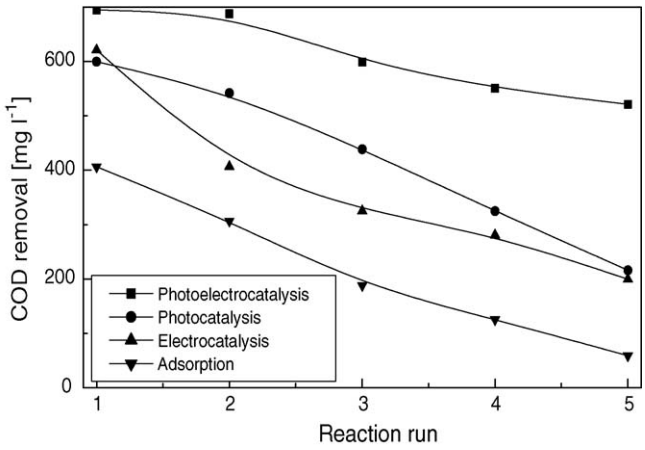

Fig. 10. COD removal for various processes for consecutive five runs.

694.7, 687.3, 598.6, 550.5, and 521.0 mg L^{-1}, respectively. By evaluating the data, it is found that all COD removal values in each run were higher than that of photoelectrocatalytic reactor without hollow quartz tubes. Moreover, the differences in COD removal in two photoelectrocatalytic reactors were obtained as 7.6, 7.03, 62.1, 65.5, and 100.0 mg L^{-1} for the five consecutive runs. The changed trend is that the differences in COD removal became larger with increase the number of runs, though COD removals decrease with increase the number of runs both in two photoelectrocatalytic reactors. Thus, we can conclude that the hollow quartz tubes play an important role in the three-dimensional electrode–hollow quartz tubes photoelectrocatalytic reactor, and a good positive correlation also was reached between the UV light distribution in the reactor and the COD removal efficiency. That is, the design of the novel photoelectrocatalytic reactor can successfully solve the drawback of UV light distribution existed in packed-bed photoelectrocatalytic reactors.

3.4. Synergetic removal of oxalic acid in the photoelectrocatalytic reactor

The efficiencies of COD removal from simulated wastewater containing oxalic acid were measured at four different processes, that is photoelectrocatalytic, photocatalytic, electrochemical, and adsorption processes, and the results are shown in Fig. 10. It can be found that the COD removal decreased with the increase of the reaction runs (operation period 60 min) in all four processes. This is because the adsorption of organic pollutants onto the catalysts is the first step in the catalytic reaction, including the photoelectrocatalytic, photocatalytic, and three-dimensional electrode reaction; thus, the efficiencies of photoelectrocatalytic, photocatalytic, and three-dimensional electrode processes would be decreased with the increase of the reaction run due to the decrease of the adsorption dosage of oxalic acid onto the immobilized photoelectrocatalyst for later reaction runs in this system. Thus, as for a packed-bed reactor, the adsorption effect of oxalic acid plays an important role in the COD removal [12]. The adsorption effect of coated photocatalyst for oxalic acid must be considered at first. When the adsorption experiments were conducted consecutively for five 60-min runs, the COD removal values were respectively 406.4, 306.7, 188.4, 125.6, and 59.1 mg L^{-1}, corresponding to the COD removal efficiencies of 49.8, 37.6, 23.0, 15.4, and 7.2%, respectively. It is noted that though the COD removal efficiencies in the first and second run of adsorption is very high, the COD removal was only 59.1 mg L^{-1}, corresponding to only 7.2% COD removal efficiency in the fifth run of adsorption. When 30.0 V cell voltage was applied across the reactor without illumination, the 199.5 mg L^{-1} COD removal corresponding to 24.4% COD removal efficiency of oxalic acid was removed in the fifth run of electrochemical oxidation. For the photocatalytic degradation process alone, a 216.1 mg L^{-1} COD removal corresponding to a 26.5% COD removal efficiency of oxalic acid was obtained in the fifth run. However, both in presence of 30.0 V cell voltages and illumination, the COD removal values of 694.7, 687.3, 598.6, 550.5, and 521.0 mg L^{-1}, corresponding to the COD removal efficiencies of 85.1, 84.2, 73.3, 67.4, and 63.8%, were obtained, respectively, for consecutive five photoelectrocatalytic degradation of oxalic acid. Table 1 presents the COD removal values and removal efficiencies from simulated wastewater containing oxalic acid at four different processes

Table 1
COD removal values and efficiency for four processes after fifth run

Process	Initial COD (mg L^{-1})	COD removal (mg L^{-1})	COD removal efficiency (%)	Net COD removal efficiency (%)	SF (%)
Photoelectrocatalysis	816.6	521.0	63.8	56.6	20.1
Photocatalysis	816.6	216.1	26.5	19.3	
Electrocatalysis	816.6	199.5	24.4	17.2	
Adsorption	816.6	59.1	7.2		

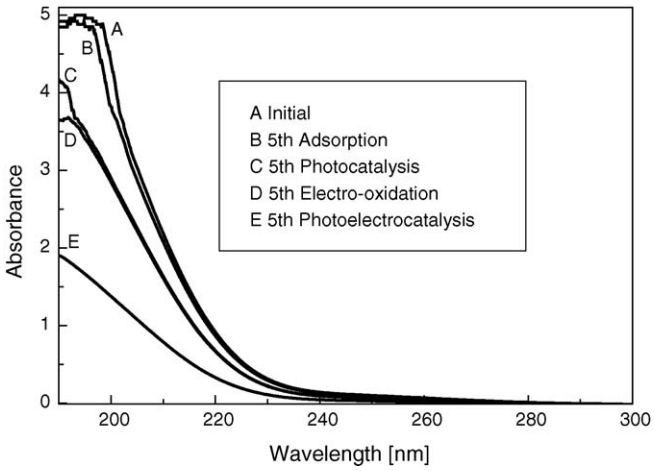

Fig. 11. UV adsorption spectra for initial and four various processes at fifth run.

for the fifth run. It is easily found that the photoelectrocatalytic process had higher COD removal efficiencies than those of the photocatalytic, electrochemical, and adsorption processes in the fifth run, and the differences in the COD removal efficiencies were 37.3, 39.4, and 56.6%, respectively. By comparing with these values, we can conclude that oxalic acid could be removed from the wastewater solution more efficiently by photoelectrocatalytic process than the other three processes alone. The UV spectrum decrease during the removal of oxalic acid at four processes can also further confirm the viewpoint. The UV spectra changes of oxalic acid in the fifth run were also presented in Fig. 11. It can be observed from the figure that the absorption peak for single photocatalytsis, electrochemical oxidation or photoelectrocatalytic processes all decreased obviously, and the curve of photoelectrocatalytic process is much lower than others.

A simple formula was put forward to assess the synergetic effect in the hybrid technology [3]. In this paper, the same formula was also used to investigate the synergetic effect in the process of photoelectrocatalytic process in this reactor. From Table 1, 63.8, 26.5, and 24.4% of COD were removed in the fifth run for the photoelectrocatalytic, photocatalytic, and electrochemical processes, respectively. By taking out 7.2% of COD removal by adsorption, the net COD removal efficiencies were 56.6, 19.3, and 17.24%, respectively for three processes. By analyzing data, it is obvious that the net removal efficiency of photoelectrochemical process (56.5%) was not only much greater than that of photocatalytic (19.3%) or electrochemical process (17.2%) alone, respectively, but also much greater than the sum of both removal efficiency of photocatalytic and electrochemical processes (36.5%). Thus, the synergetic factor (SF) obtained from the COD removal efficiency was 20.1% indicated that a clear evidence of a synergic effect existed between photocatalytic and electrochemical processes in the photoelectrochemical reactor. The existed synergic effect in the photoelectrocatalytic reactor may be attributed the capturing effect of anode bias for the photogenerated electrons and the direct or indirect electrochemical oxidation of object organic pollutants besides photoelectrocatalytic synergetic effect [3,12–15].

4. Conclusions

A novel three-dimensional electrode–hollow quartz tube photoelectrocatalytic reactor, was successfully designed by introducing the hollow quartz tubes into the three-dimensional electrode–packed-bed photoelectrocatalytic reactor, and characterized by the photocurrent enhancement and COD removal efficiency. The experimental results showed that the introduction of hollow quartz tube could well solve the UV light distribution in the photoelectrocatalytic reactor. It is found that the photoelectrocatalytic technology is more effective than the photocatalytic and the electrochemical process alone for removing organic pollutants from wastewater, and an apparent photoelectrochemical synergic effect was also observed in this photoelectrocatalytic reactor.

Acknowledgments

This work was financially supported by National Nature Science Foundation of China (40302013), Nature Science Foundation of Guangdong Province (030466) and Science & Technology Project of Guangdong Province, China (2003C34510).

References

[1] D.S. Bhatkhande, V.G. Pangarkar, A.A.C.M. Beenackers, Water Res. 37 (2003) 1223–1230.
[2] J.C. Crittenden, R.P.S. Suri, D.L. Perram, D.W. Hand, Water Res. 31 (1997) 411–418.
[3] T.C. An, Y. Xiong, G.Y. Li, C.H. Zha, X.H. Zhu, J. Photochem. Photobiol. A: Chem. 152 (2002) 155–165.
[4] A. Haarstrick, O.M. Kut, E. Heinzle, Environ. Sci. Technol. 30 (1996) 817–824.
[5] N.J. Peill, M.R. Hoffmann, Environ. Sci. Technol. 32 (1998) 398–404.
[6] N.J. Peill, M.R. Hoffmann, Environ. Sci. Technol. 30 (1996) 2806–2812.
[7] K. Hofstadler, R. Bauer, S. Novalic, G. Helsler, Environ. Sci. Technol. 28 (1994) 670–674.
[8] K. Ray, Environ. Energy Eng. 44 (1998) 477–483.
[9] I.M. Butterfield, P.A. Christensen, A. Hamnett, K.E. Shaw, G.M. Walker, S.A. Walker, J. Appl. Electrochem. 27 (1997) 385–395.
[10] J.M. Kesselman, N.S. Lewis, M.R. Hoffmann, Environ. Sci. Technol. 31 (1997) 2298–2302.
[11] K. Vinodgopal, S. Hotchandani, P.V. Kamat, J. Phys. Chem. 97 (1993) 9040–9044.
[12] T.C. An, X.H. Zhu, Y. Xiong, Chemosphere 46 (2002) 897–903.
[13] T.C. An, W.B. Zhang, X.M. Xiao, G.Y. Sheng, J.M. Fu, X.H. Zhu, J. Photochem. Photobiol. A: Chem. 161 (2004) 233–242.
[14] T.C. An, X.H. Zhu, Y. Xiong, J. Envion. Sci. Health 36A (2001) 2069–2083.
[15] W.B. Zhang, T.C. An, X.M. Xiao, G.Y. Sheng, J.M. Fu, M.C. Cui, G.Y. Li, Appl. Catal. A: Gen. 255 (2003) 221–229.
[16] M.F.J. Dijkstra, H. Buwalda, A.W.F. De-Jong, A. Michorius, J.G.M. Winkelman, A.A.C.M. Beenackers, Chem. Eng. Sci. 56 (2001) 547–555.
[17] K. Vinodgopal, U. Stafford, K.A. Gray, P.V. Kamat, J. Phys. Chem. 98 (1994) 6797–6803.
[18] A. Wahl, M. Ulmann, A. Carroy, J. Augustynski, J. Chem. Soc. Chem. Commun. 19 (1994) 2277–2278.
[19] M.W. Peterson, J.A. Turner, A.J. Nozik, J. Phys. Chem. 95 (1991) 221–225.
[20] A.J. Bard, J. Photochem. 10 (1979) 59–75.

[21] S.A. Walker, P.A. Christensen, K.E. Shaw, G.M. Walker, J. Electroanal. Chem. 393 (1995) 137–140.
[22] A. Wahl, M. Ulmann, A. Carroy, B. Jermann, M. Dolata, P. Kedzierzawski, C. Chatelain, A.A. Monnier, J. Electroanal. Chem. 396 (1995) 41–51.
[23] B. Kraeutler, A.J. Bard, J. Am. Chem. Soc. 100 (1978) 2239–2240.
[24] A.J. Bard, Science 207 (1980) 139–144.
[25] K. Vinodgopal, I. Bedja, P.V. Kamat, Chem. Mater. 8 (1996) 2180–2187.
[26] J.A. Byrne, B.R. Eggins, J. Electroanal. Chem. 457 (1998) 61–72.
[27] Y.X. Li, G.X. Lu, S.B. Li, Appl. Catal. A: Gen. 214 (2001) 179–185.
[28] R.J. Candal, W.A. Zeltner, M.A. Anderson, Environ. Sci. Technol. 34 (2000) 3443–3451.